Lab on a Chip

PAPER

View Article Online
View Journal | View Issue



Cite this: *Lab Chip*, 2026, **26**, 193

# Modeling the effects of radiation on neurogenesis using an *in vitro* neurogenic niche approach

Laura Nicoleti Zamproni,[ab] Julia Rogal,[bcd] Polyxeni Nikolakopoulou,[bc] Klas Blomgren,[ef] Marimélia Aparecida Porcionatto [a] and Anna Herland *[bcd]

Received 20th May 2025,
Accepted 17th November 2025

DOI: 10.1039/d5lc00498e

rsc.li/loc

Radiation-induced neurocognitive dysfunction after brain radiotherapy is a growing concern among the increasing numbers of long-term cancer survivors, particularly in children. This dysfunction significantly impacts memory, learning, and overall quality of life. Neural stem and progenitor cells (NSPCs) play a vital role in maintaining neurogenesis and plasticity, processes essential for memory formation and cognitive resilience. Currently, no effective treatments exist, highlighting the urgent need for strategies to mitigate these effects. One potential contributing factor to this dysfunction is the depletion or dysregulation of NSPCs following radiation. Here, we developed an *in vitro* microfluidic neurogenic niche setup to investigate how non-irradiated NSPCs respond to the inflammatory secretome produced by irradiated human fetal astrocytes (HFA) and human brain microvascular endothelial cells (HBMEC). NSPCs viability was dose-dependently affected when exposed to conditioned media from irradiated cells. Notably, NSPCs exposed to conditioned media from cells irradiated at 2 Gy and 8 Gy exhibited increased expression of *SOX9* and *S100B*, respectively, suggesting a shift toward a gliogenic fate. Our findings suggest that this microfluidic model is valuable for exploring radiation-induced neurocognitive dysfunction and identifying potential therapeutic targets.



## Introduction

The incidence of central nervous system (CNS) tumors has increased in recent decades.[1] In 2018, the reported incidence of CNS tumors was approximately 3.5 per 100 000 people.[2] Given the challenges posed by the blood–brain barrier (BBB) hindering the effective delivery of chemotherapeutic agents to the tumor, and the often incomplete surgical removal,[3] radiation therapy (RT) remains a primary treatment modality for CNS tumors and brain metastases in both pediatric and adult patients.[4] Even though the main objective of RT is to eliminate tumor cells without causing harm to surrounding normal tissues, unavoidable radiation exposure of healthy tissue can lead to brain cell damage.[5] Consequently, RT is associated with various complications, with neurocognitive impairment arguably being the most debilitating, such as learning problems, memory dysfunction, and progressive dementia.[6] Radiation-induced neurocognitive dysfunction has garnered attention, given the rising prevalence of CNS tumors and the growing population of long-term cancer survivors.[7] Currently, there are no effective treatments for that condition, highlighting the need to develop new strategies for enhancing patients' quality of life.[8]

While the detailed mechanisms of radiation-induced neurocognitive dysfunction are not fully understood, existing evidence points to neurogenesis inhibition as one such mechanism.[9–11] Neural stem and progenitor cells (NSPCs) rely heavily on their local microenvironment, the neurogenic niche, which plays a central role in regulating stem cell biology. This niche consists of structural, nutritional, and signaling support provided by niche-resident cells that tightly control NSPCs proliferation, differentiation, and survival.[12] Among these, astrocytes and endothelial cells are well-recognized as key regulators of neurogenesis, influencing NSPCs function through a variety of paracrine and contact-mediated mechanisms.[13–15]

Following radiation exposure, complex processes—including cell death, senescence[16,17] and the production of inflammatory mediators—disrupt the neurogenic niche, ultimately leading to tissue dysfunction and cognitive deficits.[18] Radiation-damaged astrocytes and endothelial cells

[a] *Department of Biochemistry, Escola Paulista de Medicina, Universidade Federal de São Paulo, São Paulo, Brazil*
[b] *AIMES – Center for the Advancement of Integrated Medical and Engineering Sciences at Karolinska Institutet and KTH Royal Institute of Technology, Stockholm, Sweden. E-mail: anna.herland@ki.se*
[c] *Department of Neuroscience, Karolinska Institutet, Stockholm, Sweden*
[d] *Division of Nanobiotechnology, Department of Protein Science, SciLifeLab, KTH Royal Institute of Technology, Sweden. E-mail: aherland@kth.se*
[e] *Department of Women's and Children's Health, Karolinska Institutet, 17165 Stockholm, Sweden*
[f] *Pediatric Oncology, Karolinska University Hospital, 17164 Stockholm, Sweden*

produce inflammatory signals. This effect is believed to impair NSPCs proliferation and neuronal differentiation, contributing to long-term neurocognitive deficits.[2]

Addressing this damaged microenvironment and preventing secondary NSPCs damage represent viable therapeutic approaches for mitigating radiation-induced neurocognitive dysfunction. To advance this understanding, we developed an *in vitro* microfluidic neurogenic niche setup that that enables detailed studies of how non-irradiated NSPCs respond to secreted factors from irradiated astrocytes and endothelial cells, providing valuable insights that complement *in vivo* experiments. By leveraging this system, we aim to uncover the cellular and molecular pathways involved in NSPCs dysfunction and identify therapeutic targets to mitigate radiation-induced damage and its downstream effects.

## Materials and methods

### Reagents

DPBS minus $Ca^{++}$ and $Mg^{++}$ (14190144, Thermo Fisher, Waltham, Massachusetts, USA), DPBS with $Ca^{++}$ and $Mg^{++}$ (14040091, Thermo Fisher), Astrocyte Media (AM1801, ScienCell, Carlsbad, California, USA), TrypLE™ (12604013, Thermo Fisher), attachment factor protein 1× (S006100, Thermo Fisher), EGM™-2 MV Microvascular Endothelial Cell Growth Medium-2 BulletKit™ (CC-3202, Lonza, Basel, Switzerland), Endothelial Cell Growth Medium MV2 (C-22022, PromoCell, Heidelberg, Germany), DMEM: F12 Glutamax (31331-028, Thermo Fisher), N2 supplement (17502-048, Thermo Fisher), B27 serum free (11530536, Thermo Fisher), B27 minus antioxidants (10889038, Thermo Fisher), FGF (233-FB, R&D Systems, MN, USA), EGF (E9644, Sigma Aldrich, Burlington, Massachusetts, USA), PLO (P3655, Sigma Aldrich), laminin (L2020, Sigma Aldrich), defined trypsin inhibitor (DTI, R007100, Thermo Fisher), Transwells 0.4 μM microporous membrane (833932041, Sarstedt, Nümbrecht, Germany), high Pure RNA Isolation Kit (11828665001, Roche, Basel, Switzerland), high-capacity RNA-to-cDNA kit (4387406, Thermo Fisher), TaqMan probes (Applied Biosystems, California, USA), fast advanced master mix (4444557, Applied Biosystems), trypan blue (1450021, Bio-Rad, Hercules, California, USA), LEGENDplex™ Human Inflammation Panel 1 (13-plex) assay using a V-bottom plate (BioLegend, San Diego, California, USA), Alamar Blue reagent (DAL1100, Thermo Fisher), goat serum (G9023, Sigma Aldrich), Cascade Blue™ hydrazide, trisodium salt (C687, Thermo Fisher).

### Cell culture

Human neuroepithelial stem cells (NSPCs) NSPCs line (control 9: male, dual-SMAD neural induction[19,20]) were provided by the iPS Core facility (Karolinska Institute, Sweden). NSPCs were cultured and passaged in DMEM: F12 Glutamax supplemented with N2 1 : 100, B27 1 : 1000, 10 ng $mL^{-1}$ bFGF and 10 ng $mL^{-1}$ EGF – the complete media is termed N2B27 – on double coated PLO (20 μg $mL^{-1}$) and laminin (L2020, 1 : 500) flasks. Culture vessels were incubated overnight with PLO, washed thoroughly two times with DPBS (with $Ca^{++}$ and $Mg^{++}$), and then coated overnight with L2020. NSPCs were passaged at a splitting ratio of 1 : 4–1 : 5. Briefly, cells were washed with DPBS (minus $Ca^{++}$ and $Mg^{++}$) and then incubated with TrypLE™ for 3–4 min. TrypLE™ was deactivated using equal volumes of DTI and DMEM: F12 Glutamax (1 : 1 : 1), spun down at 200 g, and resuspended in N2B27. Media was replenished entirely every other day.

Human fetal astrocytes (HFA) (ScienCell, CA, USA): HFA were cultured in ScienCell astrocyte media (AM) supplemented with 2% FBS and 1% AGS (complete AM media). HFA were used in passages 6 to 9. Cells were passaged once they reached 100% confluency with a 1 : 4 ratio. Briefly, cells were washed with DPBS (minus $Ca^{++}$ and $Mg^{++}$) and then incubated with TrypLE™ for 3–4 min. The enzymatic reaction was inactivated using cell media at a ratio of 1 : 5, spun down at 200 g, and resuspended in complete AM media. No coating was used for HFA. Media was replenished entirely every other day.

Primary human brain microvascular endothelial cells (HBMEC) (Cell Systems, WA, USA): HBMEC were cultured in EGM™-2 MV Microvascular Endothelial Cell Growth Medium-2 BulletKit™ or Endothelial Cell Growth Medium MV2 in attachment factor-coated flasks. HBMEC were used in passages 8 to 11. The cells were passaged once they reached 100% confluency with a 1 : 4 ratio. Briefly, cells were washed with DPBS (minus $Ca^{++}$ and $Mg^{++}$) and then incubated with TrypLE™ for 2 min. TrypLE™ was inactivated using cell media 1 : 5, spun down at 200 g, and resuspended in complete media. Media was replenished entirely every other day.

### Radiation procedure

The radiation procedure was carried out using CIX2 X-ray cabinets (Xstrahl, GA, USA). Radiation doses were adjusted by varying the distance between the samples and the radiation source (measured in cm) and the exposure duration (Table 1). In all experiments, cells received a single radiation dose. For some experiments, cells were used immediately after irradiation. In other cases, cells were cultured for 10 days post-irradiation before experimentation.

### Viability assay

NSPCs, HFA, or HBMEC, were seeded in 96 well plates, 10 000 cells per $cm^2$, in their respective culture media and allowed to attach overnight at 37 °C, 5% $CO_2$. On the next day, a radiation procedure was performed. The respective culture media were changed every other day. Cell viability was measured on the different endpoints (2, 7, or 14 days) using Alamar Blue reagent (resazurin). Cell media was removed, and Alamar Blue 10% was added to the wells. Plates were incubated at 37 °C for 4 hours. After that time, fluorescence (excitation/emission: 560/590) was measured in a plate reader (Infinite, M1000 pro, Tecan, Männedorf, Switzerland). Quantification was done to establish the

 

Table 1 CIX2 X-ray cabinets parameters. All recipes were calculated using a 3 mm aluminum filter, 195 kV, 10 mA

| Radiation (Gy) | Distance from radiation source (cm) | Time |
|---|---|---|
| 0.5 | 60 | 50 seconds |
| 1 | 60 | 1 minute & 40 seconds |
| 2 | 50 | 2 minutes & 19 seconds |
| 4 | 40 | 2 minutes & 58 seconds |
| 8 | 40 | 5 minutes & 56 seconds |



fluorescence in the non-irradiated (NI) groups as 100% viable cells. The other conditions tested were expressed in percentage compared to the NI group.

### Immunocytochemistry

Cells were washed with DPBS (with $Ca^{++}$ and $Mg^{++}$) and fixed with 4% PFA for 10 min at room temperature. After washing twice with DPBS (with $Ca^{++}$ and $Mg^{++}$), cells were incubated with blocking buffer (10% goat serum) and 0.1% Triton X-100 in DPBS (with $Ca^{++}$ and $Mg^{++}$). Primary antibody incubation was done in dilution buffer (10% blocking buffer) overnight at 4 °C. After 3× washes in DPBS (with $Ca^{++}$ and $Mg^{++}$), cells were stained with DAPI (4′,6′-diamino-2-fenil-indol) (1 : 2000) plus appropriate secondary antibody in dilution buffer at room temperature for an hour. Cells were washed 3× and imaged with a cell observer fluorescent microscope (Zeiss, Oberkochen, Germany). Images were processed using ImageJ (https://imagej.net). A detailed list of the antibodies used can be found in Table S1.

### mRNA analysis

Cells were collected and lysed at 6 hours, 24 hours, and 14 days post-irradiation (DPI); total RNA was extracted using the High Pure RNA Isolation Kit (Roche, Basel, Switzerland); cDNA synthesis was carried out using the high-capacity RNA-to-cDNA kit (Thermo Fisher) on a thermal cycler. TaqMan probes of interest (Applied Biosystems, CA, USA) were incubated with cDNA samples in Fast Advanced Master Mix (Applied Biosystems). Samples were run on QuantStudio™ 5 Real-Time PCR System. Target genes were normalized for quantification using the geometric mean of Beta-actin (*ACTB*) and glyceraldehyde 3-phosphate dehydrogenase (*GAPDH*). The threshold cycles (Ct) were determined for each sample. The relative expression of mRNA was calculated using the $2^{-\Delta\Delta Ct}$ method.[21] A list of the TaqMan probes used can be found in Table S2.

### Permeability assay in Transwells

To assess the permeability of HBMEC after irradiation, 50 000 cells were seeded into the upper chamber of a Transwell (TW). TWs were irradiated and permeability was assessed at specific time points (24 hours, 3 days, and 11 days post-irradiation). For the permeability assay, media in the TW system was refreshed (200 μL upper chamber, 800 μL bottom chamber), and the plates were incubated at 37 °C to equilibrate. Next, 100 μL of media from the upper chamber was replaced with 100 μL of media containing 200 μg $mL^{-1}$ of Cascade blue (CB) dye. The plates were then placed on an orbital shaker at 150 rpm for 4 hours at 37 °C to facilitate dye movement. After 4 hours, 100 μL of media from the bottom chamber was carefully collected and transferred to a 96-well plate. Fluorescence intensity was measured at an excitation wavelength of 400 nm and an emission wavelength of 420 nm using the Infinite M1000 pro (Tecan). A standard curve of CB was used to calculate the dye concentration in the bottom chamber, providing a measure of HBMEC permeability.

### NSPC viability in N2B27 medium without both FGF and EGF

To evaluate how irradiated cells affect the proliferative behavior of NSPCs, we established a coculture system using a TW. In this setup, TWs containing irradiated HFA or HBMEC were placed in a 24-well plate, where non-irradiated (NI) NSPCs were seeded at the bottom. The culture medium was DMEM: F12 Glutamax supplemented with N2 1 : 100, B27 minus anti-oxidants (AO) 1 : 100 without FGF and without EGF, meaning that the only trophic support for the NSPCs came from the cells in the TW. NSPCs viability was measured using the Alamar Blue assay at designated time points.

To design the above mentioned experiment and determine the appropriate initial seeding density of NSPCs, we first assessed how NSPCs grow in N2/B27 medium without growth factors. NSPCs were seeded at 20 000 cells per $cm^2$ and allowed to attach overnight. Initial viability was measured using 10% Alamar Blue (4-hour incubation), followed by a media change to N2/B27 without growth factors. The Alamar Blue assay was repeated at specific time points (3, 5, 7, and 10 days).

As shown in Fig. S1, the growth curve indicates that NSPCs continued to proliferate up to 3 days after growth factor removal but began to die thereafter. Therefore, for experiments with an acute endpoint (up to 3 days), we seeded a lower density of NSPCs, allowing sufficient space for proliferation. Conversely, for long-term experiments, we seeded a higher initial density to compensate for the natural cell death observed over time.

### Coculture in Transwells (TW)

**1. Irradiated HFA × NI NSPCs.** NSPCs were plated at the bottom of a 24-well plate at a density of 5000 cells per $cm^2$. HFA were plated inside the TW (100 000 cells per

TW) (0.4 μm microporous membrane). On the next day, after both seedings, HFA in TW were irradiated (2 Gy or 8 Gy) and placed on the top of NI NSPCs immediately after the procedure. N2B27 (regular B27 was changed to minus AO and increased to 1 : 100) without growth factors (FGF and EGF) was used in the top and bottom chambers. The system was maintained for three days at 37 °C. After three days, NSPC viability was verified by Alamar Blue reagent. Cell media was removed, and Alamar Blue 10% was added to the wells. Plates were incubated at 37 °C for 4 hours. After that time, fluorescence (excitation/emission: 560/590) was measured in a plate reader (Infinite, M1000 pro, Tecan).

**2. Irradiated HBMEC × NI NSPCs.** NSPCs were plated at the bottom of a 24-well plate at a density ratio of 5000 cells per $cm^2$. HBMEC were plated inside the TW (100 000 cells per TW) (0.4 μm microporous membrane). On the next day, after both seedings, HBMEC in TW were irradiated (2 Gy or 8 Gy) and placed on the top of NI NSPCs immediately after the procedure. N2B27 (1 : 100, minus AO without FGF and EGF) was used in the bottom chamber. A human endothelial serum-free medium (Thermo Fisher) plus B27 antioxidant-free (1 : 100) was used in the top chamber. The system was maintained for three days at 37 °C. After three days, NSPCs viability was verified by Alamar Blue reagent. Cell media was removed, and Alamar Blue 10% was added to the wells. Plates were incubated at 37 °C for 4 hours. After that time, fluorescence (excitation/emission: 560/590) was measured in a plate reader (Infinite, M1000 pro, Tecan).

**3. HFA 10 days post-irradiation × NI NSPCs.** HFA were plated in six-well plates at 5000 cells per $cm^2$. On the next day, cells were irradiated once (2 Gy or 8 Gy). After the procedure, cells were cultured in AM media for ten days. After that time HFA were seeded inside TW (100 000 cells per TW). NSPCs were plated at the bottom of a 24-well plate at a 20 000 cells per $cm^2$ density. The day after NSPCs seeding, HFA in TW was placed on top of NSPCs. N2B27 (1 : 100, minus AO, without FGF and EGF) was used in both the top and bottom chambers. The TW system was maintained for 14 days at 37 °C. On day 14, NSPC viability was verified by the Alamar Blue reagent. Cell media was removed, and Alamar Blue 10% was added to the wells. Plates were incubated at 37 °C for 4 hours. After that time, fluorescence (excitation/emission: 560/590) was measured in a plate reader (Infinite, M1000 pro, Tecan).

### Microfluidic neurogenic niche setup

The microfluidic chips, manufactured by Cell Box Labs (Latvia), consist of two channels PDMS channels separated by a membrane PET membrane. The top channel measures 1200 ± 25 μm, while the bottom channel is 982 ± 25 μm. The membrane (IP4IT, Belgium, catalog IT41P1000M25/610M103) has a pore size of 1 μm, a pore density of $1.6 \times 10^6$ $cm^{-2}$, and a thickness of 24 μm. The microfluidic circuit operates with an Ismatec IPC pump featuring 16 channels, steel connectors (21G), and dispensing needles (21G). PharmMed peristaltic tubing with an inner diameter of 0.25 mm and extension tubing of 0.51 mm completes the system. For seeding the neurogenic niche chip the channels were coated with collagen IV (400 μg $mL^{-1}$) and fibronectin (100 μg $mL^{-1}$) overnight. Both channels of the chip were rinsed with DPBS (with $Ca^{++}$ and $Mg^{++}$) and then with AM before seeding cells. For HFA in the brain channel of a chip, a density of $4 \times 10^6$ cells per mL in AM was seeded on the basal channel of the chip (15 μL). The device was flipped immediately to allow the HFA to adhere to the collagen IV/fibronectin-coated PET membrane and then incubated at 37 °C for one hour. Then, $8 \times 10^6$ cells per mL of HBMEC were seeded in the apical channel in EGM™ -2 MV (15 μL). Three types of chips were constructed: 1) 'NI Chip' containing NI HFA and NI HBMEC, 2) '2 Gy I Chip' containing 2 Gy irradiated HFA and HBMEC, cultivated for 10 days to acquire persistent inflammatory characteristics, and 3) '8 Gy I Chip' containing 8 Gy irradiated HFA and HBMEC, cultivated for 10 days to acquire persistent inflammatory characteristics. Chips seeded with cells were maintained in the incubator for 24 hours, with EGM™ -2 MV media changing every 12 hours in both channels. On the second day of cell seeding into the microfluidic device, both channels were connected to peristaltic pumps and the medium flowed through the channels (60 μL $h^{-1}$) to allow the cell layers to adjust to flow conditions. EGM™ -2 MV was used in the vascular channel, N2/B27 (1 : 100, minus AO, without FGF and EGF) was used in the brain channel. One day later, the circuit was connected to 10 000 NSPCs per $cm^2$ flasks (containing 2 mL of N2/B27, 1 : 100, minus AO, without FGF and EGF). From this moment, NSPCs were fed only by the media flowing in the chip. Every day, 1.5 mL of media were removed from each flask. On day 7, NSPCs were detached as previously described, replated in flasks at 20 000 NSPCs per $cm^2$ density, and reconnected to the chips. On day 14, NSPCs viability was verified using the Alamar Blue reagent method. After the experiment was finished, RNA was extracted from NSPCs as previously described.

### Chip permeability

To determine barrier function in the chip, the CB was included (100 μg $mL^{-1}$) in the vascular channel and flowed (60 μL per hour) through. The concentrations of the tracers were measured after the experiment (22 hours) in the affluents and effluents of the brain and vascular channels using a CB standard curve.

### Permeability assay in Transwells (TW) for comparing with chip permeability

The media in the TW system was refreshed. The upper chamber received 200 μL of fresh media, while the bottom chamber received 800 μL, and the plates were incubated at 37 °C to equilibrate. Next, 100 μL of media from the upper chamber was replaced with 100 μL of media containing CB

 

200 μg $mL^{-1}$ (final concentration in the upper chamber is 100 μg $mL^{-1}$). The plates were then incubated for 22 hours at 37 °C (no shaking). After 22 hours, 100 μL of media from the bottom chamber was carefully collected and transferred to a 96-well plate. Fluorescence intensity was measured at an excitation wavelength of 400 nm and an emission wavelength of 420 nm using the Infinite M1000 pro (Tecan). A standard curve of CB was used to calculate the dye concentration in the bottom chamber.

### LEGENDplex analysis

To measure cytokine levels in the conditioned media from the neural chamber from the chips, we used the LEGENDplex™ Human Inflammation Panel 1 (13-plex), a multiplex bead-based assay, enabling the simultaneous detection of 13 inflammatory cytokines: IL1B, IFNA2, IFNG, TNFA, MCP1 (CCL2), IL6, CXCL8 (IL8), IL10, IL12p70, IL17A, IL18, IL23, and IL33. We pooled media from three chips between days 17 and 21 post-irradiation. The pooled samples were analyzed in quadruplicate. The analysis was carried out using the BD FACSCanto™ II Flow Cytometry System (BD, Franklin Lakes, NJ, USA), which identified bead types and measured fluorescence intensity. Data were processed using LEGENDplex™ software to generate standard curves and quantify cytokine concentrations.

### mRNA analysis of NSPCs receiving the chip effluent

We conducted five independent chip assays. Total RNA from the NSPCs in the flasks was extracted using the High Pure RNA Isolation Kit (Roche, Basel, Switzerland). The mRNA production, and qPCR were performed as previously described. Delta threshold cycles (ΔCt) were determined for each sample by subtracting the target gene threshold cycle (Ct) minus the geometric mean of *ACTB* and *GAPDH*. The delta delta Ct (ΔΔCt) for each target gene was determined by comparing the ΔCt of experimental samples to that of control within the same experiment. Fold change (FC) was computed using the 2^(−ΔΔCt) method.[21] Statistical analysis was applied to five FCs obtained for each condition.

### Statistical analysis

Statistically significant differences were evaluated by one-way ANOVA followed by Tukey post-test, unless otherwise stated. Results are expressed as mean ± standard error of the mean and were considered significant if $p < 0.05$.

## Results

### NSPC viability is affected by radiation in a dose-dependent manner

Our first goal was to verify the radiosensitivity of the different cell types. NSPCs, HFA, and HBMEC were irradiated (0.5 to 8 Gy), and a resazurin mitochondrial reduction-based assay was performed to estimate cell viability.

NSPCs viability was drastically impaired two days post-irradiation (DPI), even the lowest dose 0.5 Gy induced a statistically significant decrease in NSPC viability. A reduction of 50 and 80% of NSPCs viability was seen in 2 Gy and 8 Gy-irradiated groups, respectively (Fig. 1A). These effects remain at 7 DPI, showing that even low doses of radiation can be highly harmful to NSPCs (Fig. 1B).

A different pattern of behavior was observed for HFA: HFA viability showed no change for any of the doses two DPI (Fig. 1C). At 7 DPI, HFA viability was nearly 80% in both 2 and 8 Gy-irradiated HFA compared to non-irradiated (NI) HFA (Fig. 1D). On 14 DPI, the 8 Gy-irradiated group presented 65% viability compared to the NI (Fig. 1E).

Finally, HBMEC showed no significant change in cell viability in any endpoints (Fig. 1F–H).

### HFA acquires an inflammatory phenotype after irradiation

The next step was verifying HFA' and HBMEC' radiation-induced phenotypes. HFA irradiated with 8 Gy appeared to exhibit hypertrophy within the following 12 DPI, as indicated by the arrows in Fig. 2A. The cell nuclei are larger, and the cell bodies appear more triangular in shape. Aquaporin-4 (AQP4), a water channel expressed on astrocytic endfeet[22] was not different among the groups. Intercellular adhesion molecule (ICAM) fluorescence was significantly higher in the 8 Gy-irradiated group 12 DPI (Fig. 2B and C). ICAM is an adhesion molecule upregulated upon inflammatory stimulation. These findings also were in agreement with that 8 Gy irradiated HFA had higher RNA expression levels of Interleukin 1 beta (*IL1B*) and Interleukin 6 (*IL6*) 24 hours post-irradiation (Fig. 2D and E); and high levels of *IL6* expression were sustained for 14 DPI (Fig. 2F). On the other hand, 2 Gy-irradiated HFA increased interleukin 10 (*IL10*) expression in the 14 DPI (Fig. 2G). The proliferation marker *MKI67* expression decreased drastically in 8 Gy-irradiated HFA 14 DPI (Fig. 2H). The entire inflammatory profile of irradiated HFA within six hours, one day and 14 DPI can be seen in Fig. S2.

### HBMEC also alter their phenotype after irradiation

HBMEC did not show altered viability after irradiation, but as expected,[23] radiation impaired endothelial barrier function. Cascade blue (CB) dye permeability was increased in the 8 Gy irradiated group at 3DPI and for 2 and 8 Gy at 11 DPI for HBMEC in TW monocultures. (Fig. 3A–C). We noted reduced vascular endothelial cadherin (VECAD) fluorescence in 2 and 8 Gy-irradiated groups at 3 DPI (Fig. 3D and E). Similar to the observation in HFA, HBMEC also presented evident hypertrophy (arrows) by 12 DPI (Fig. 3D).

On a gene expression level, *TNFA* (tumor necrosis factor alfa) was increased in the 2 Gy-irradiated group, 6 hours post-irradiation (HPI, Fig. 3F). In 8 Gy-irradiated HBMEC, *IL6* expression increased in the first 6 HPI (Fig. 3G) and was sustained for 1 DPI (Fig. 3H), while increased *IL1B* was only seen 14 DPI (Fig. 3I). The entire inflammatory profile of

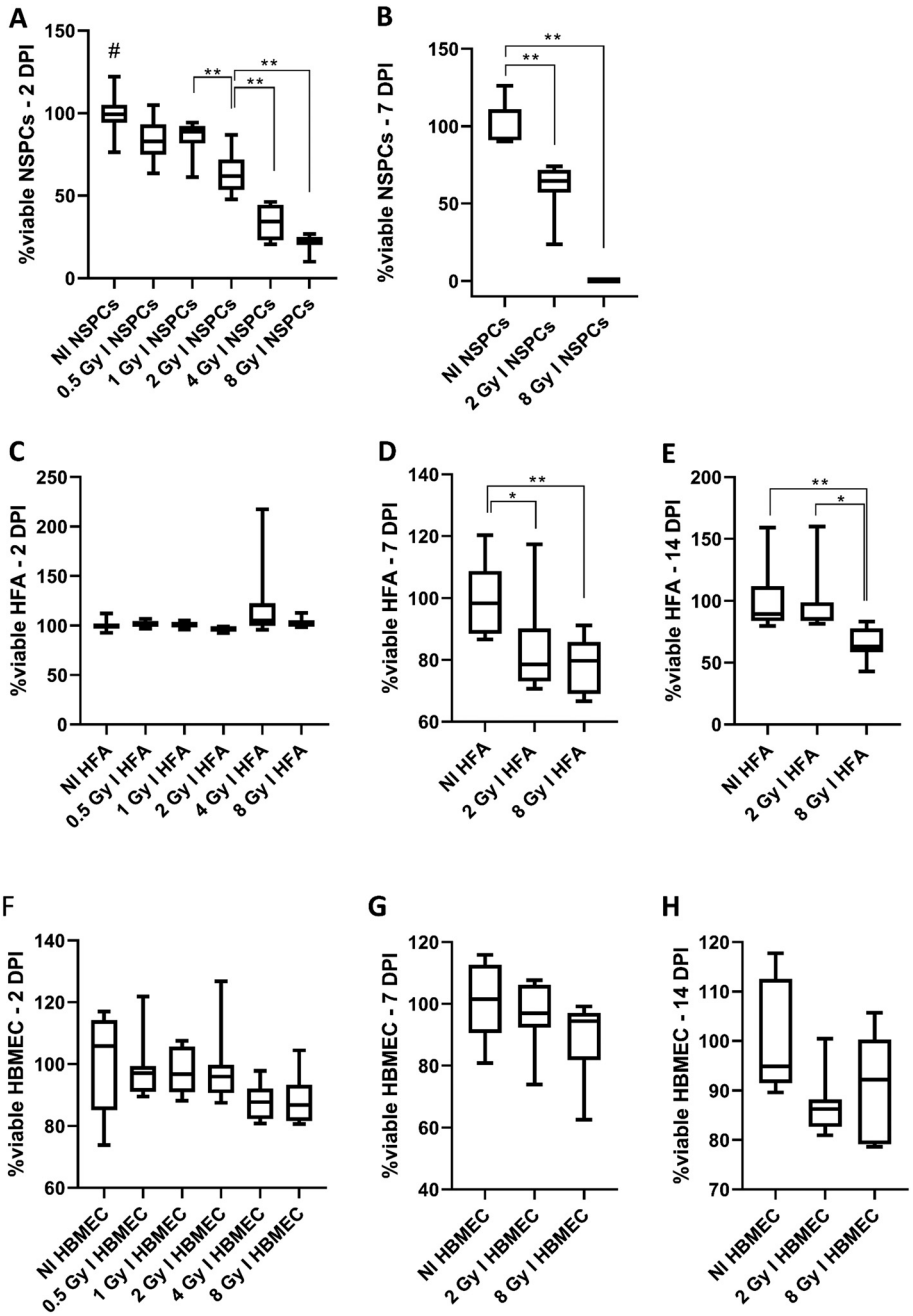


**Fig. 1** Cell viability in response to radiation. Viability was measured as the fluorescence of Alamar Blue. Quantification was done to establish the fluorescence in the non-irradiated (NI) groups as 100% viable cells. The other conditions tested were expressed as a percentage compared to the NI group. (A) NSPC viability 2 DPI. The NI group was statistically different ($p < 0.05$) when compared to all other groups. This was represented by the # symbol. (B) NSPC viability 7 DPI. (C) HFA viability 2 DPI, (D) 7 DPI and (E) 14 DPI. (F) HBMEC viability 2, (G) 7, and (H) 14 DPI. Boxes represent the first and third quartiles, while lines represent the maximum and minimum values. # = $p < 0.05$ when compared to all other groups, * = $p < 0.05$, ** = $p < 0.01$, one-way ANOVA plus Tukey multiple comparisons test, $n$ = 8 to 10 samples per group. NSPCs: neural stem and progenitor cells, HFA: human fetal astrocytes, HBMEC: human brain microvascular endothelial cells, NI: non-irradiated, I: irradiated, Gy: gray; DPI: days post-irradiation.

irradiated HBMEC in six hours, one DPI and 14 DPI can be seen in Fig. S3.

### Irradiated HFA enhance NSPC proliferation within 3 days

After confirming radiation-induced changes in both phenotypes and gene expression of HFA and HBMEC, we aimed to determine whether these changes could influence the trophic support these cells provide to non-irradiated neural stem and progenitor cells (NI NSPCs).

To test this, we first examined how irradiated HFA (I HFA) affect NSPC proliferation. Using a TW coculture system, we placed irradiated HFA in the upper chamber of a 24-well plate, with NI NSPCs in the lower chamber. Importantly, the

 

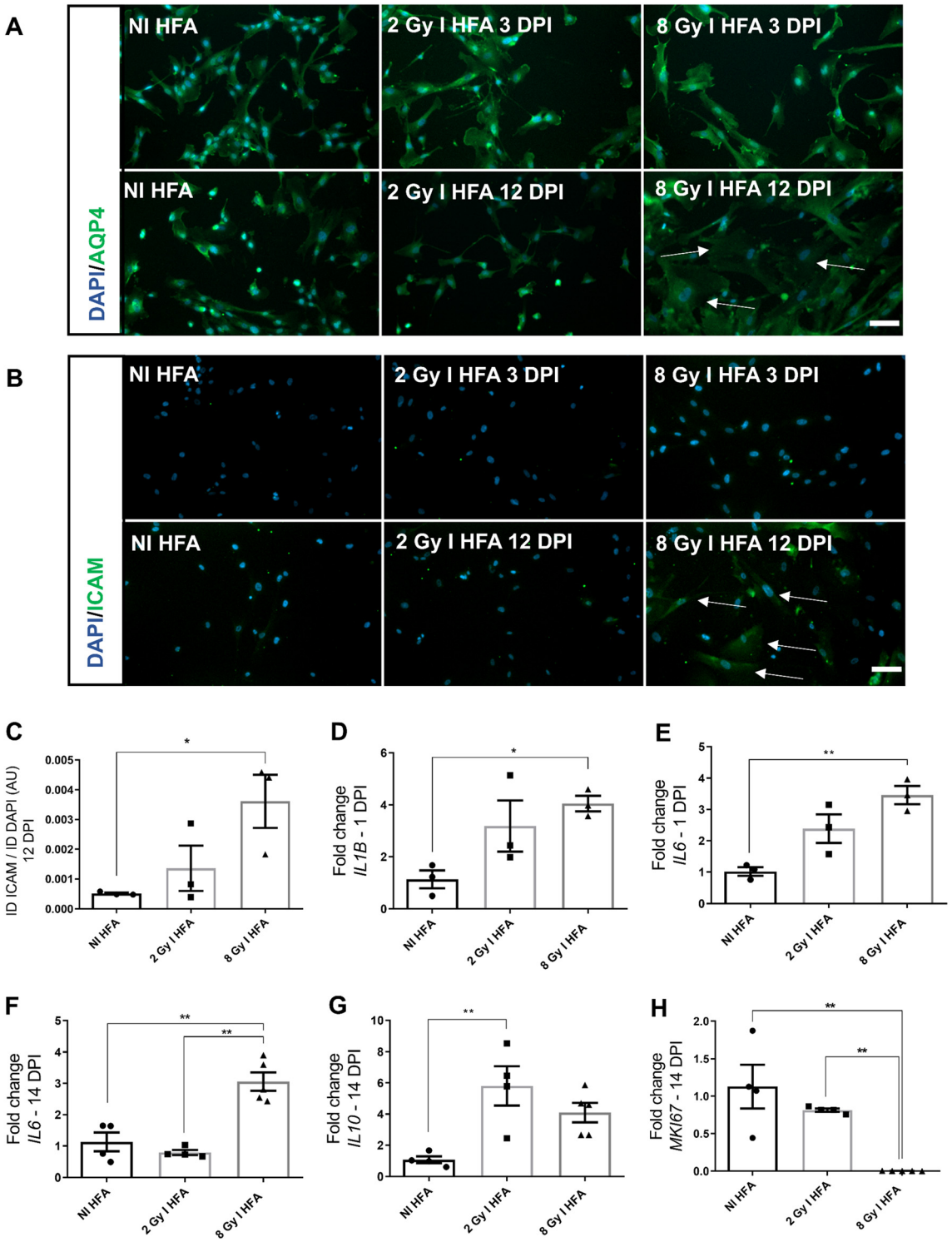


**Fig. 2** Immunocytochemistry and gene expression profile analysis of HFA on different time points post-irradiation. (A) Aquaporin 4 immunostaining. Arrows indicate the presence of hypertrophic cells in the 8 Gy irradiated HFA, 12 DPI. Scale bar = 100 μm. (B) ICAM immunostaining. Arrows indicating cells overexpressing ICAM in 8 Gy irradiated HFA, 12 DPI. Scale bar = 100 μm. (C) Quantification of ICAM fluorescence in 12 DPI. Results are expressed as the integrated density of the green channel corrected by the number of cells (DAPI integrated density). $N = 3$ (D) *IL1B* gene expression in irradiated HFA in 1 DPI. $N = 3$ (E) IL6 gene expression in irradiated HFA in 1 DPI. $N = 3$ (F) *IL6* gene expression in irradiated HFA in 14 DPI. $N = 4$ to 5 (G) *IL10* gene expression in irradiated HFA in 14 DPI. $N = 4$ to 5 (H) *MKI67* gene expression in irradiated HFA in 14 DPI. $N = 4$ to 5. * = $p < 0.05$, ** = $p < 0.01$, one-way ANOVA plus Tukey multiple comparisons test. HFA: human fetal astrocytes, NI: non-irradiated, I: irradiated, Gy: gray, *IL10*: interleukin 10, *IL6*: interleukin 6, *IL1B*: interleukin one beta, *MKI67*: a marker of proliferation Ki-67. AQP4: aquaporin 4, ICAM: intercellular adhesion molecule, ID: integrated density, AU: arbitrary units, DPI: days post-irradiation.

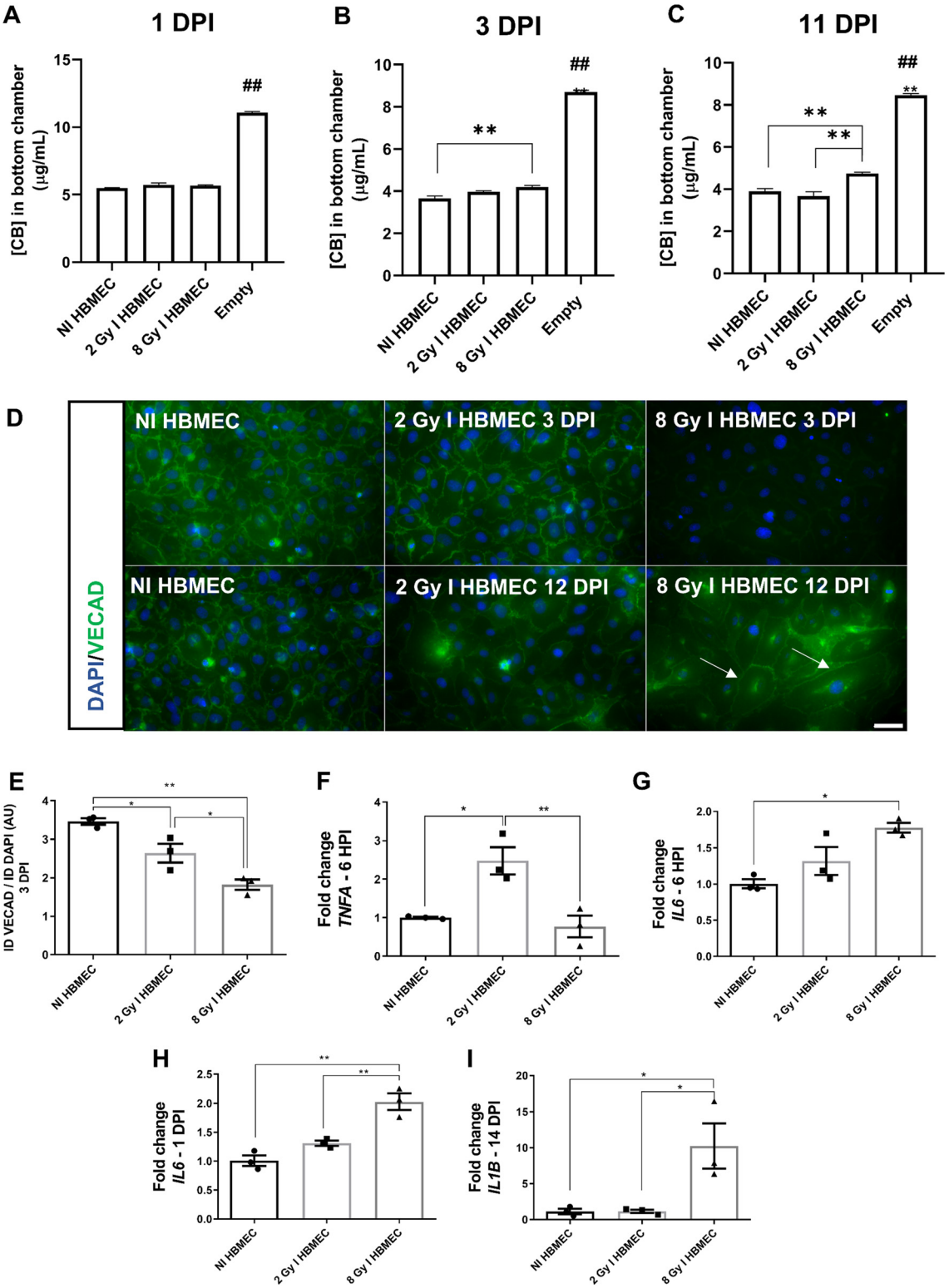


**Fig. 3** Radiation-induced effects on endothelial barrier function and inflammatory profile in HBMEC. (A–C) CB permeability is increased in the 8 Gy-irradiated group at 3 and 11 DPI. ## = $p < 0.01$ compared to all other groups, ** = $p < 0.01$, ANOVA plus Tukey *post hoc* test, $n = 6$ (D) VECAD immunostaining. Arrows indicate the presence of hypertrophic cells in the 8 Gy irradiated HBMEC, 12 DPI. Scale bar = 50 µm. (E) Quantification of VECAD fluorescence by 3 DPI. Results are expressed as the integrated density of the green channel corrected by the number of cells (DAPI integrated density). $N = 3$ (F) *TNFA* gene expression in irradiated HBMEC in 6 HPI. $N = 3$ (G) *IL6* gene expression in irradiated HBMEC in 6 HPI. $N = 3$ (H) *IL6* gene expression in irradiated HBMEC in 1 DPI. $N = 3$ (I) *IL1B* relative expression in irradiated HBMEC by 14 DPI. $N = 3$. * = $p < 0.05$, ** = $p < 0.01$, ANOVA plus Tukey *post hoc* test. HBMEC: human brain microvascular endothelial cells, NI: non-irradiated, I: irradiated, Gy: gray, *IL6*: interleukin 6, *IL1B*: interleukin one beta, *TNFA*: tumor necrosis factor alfa, VECAD: vascular endothelial cadherin, ID: integrated density, AU: arbitrary units, HPI: hours post-irradiation, DPI: days post-irradiation, CB: Cascade blue.

culture medium lacked fibroblast growth factor (FGF) and epidermal growth factor (EGF), so the only sources of trophic support for the NSPCs were factors secreted by the HFA.

Compared to the control group, which had an empty TW (no HFA), the presence of HFA increased the number of viable NSPCs, suggesting that the HFA secreted trophic factors that promoted NSPCs survival. Notably, irradiated HFA exposed to 8 Gy of radiation further increased NSPCs numbers compared to non-irradiated HFA (NI HFA). This effect was observed after 3 days of coculture (Fig. 4A).

### HFA 10 days post-irradiation and their impact on NSPC proliferation over 14 days

Next, we irradiated HFA once and cultured them for 10 days to establish a persistent inflammatory phenotype. HFA were then seeded in a TW and cocultured with NSPCs for an additional 14 days. To promote NSPCs survival during this culture period, we increased their initial density.

After 14 coculture days, NSPCs cocultured with either NI HFA or 2 Gy irradiated HFA exhibited a higher cell count compared to the empty TW group, highlighting the trophic support provided by the HFA (Fig. 4B). However, no significant difference in cell count was observed between the group cocultured with 8 Gy irradiated HFA and the empty TW group.

### Irradiated HBMEC promote NSPC proliferation in 3 days

Since HBMEC are known to provide trophic support to NSPCs in the neurogenic niche, we applied the same protocol used for HFA to HBMEC. In this experiment,

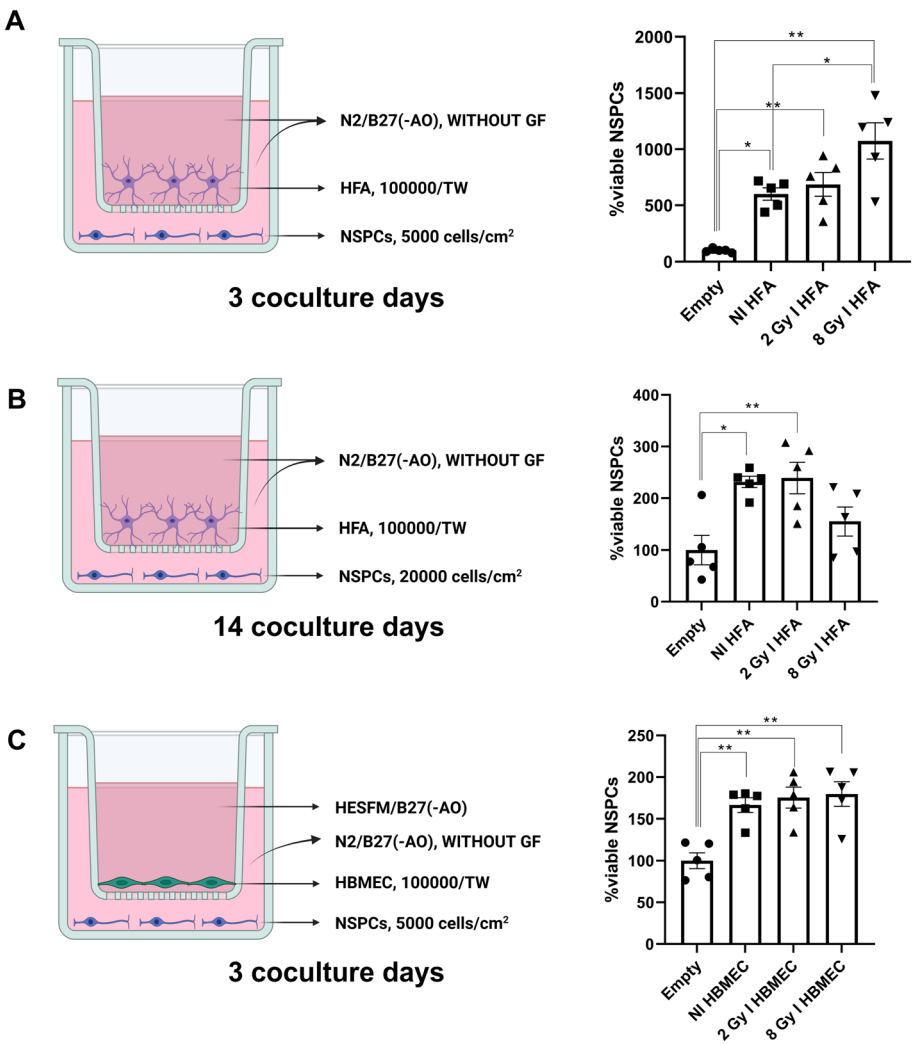


**Fig. 4** Coculture assays using a Transwell system. (A) Coculture of immediately irradiated HFA with non-irradiated neural stem and progenitor cells (NI NSPCs). $N = 5$. (B) Coculture of HFA 10 DPI with NI NSPCs. $N = 5$. (C) Coculture of immediately irradiated human brain microvascular endothelial cells (HBMEC) with NI NSPCs. $N = 5$. Statistical significance is indicated as follows: * = $p < 0.05$, ** = $p < 0.01$ (ANOVA followed by Tukey *post hoc* test). NSPCs: neural stem and progenitor cells, HFA: human fetal astrocytes, HBMEC: human brain microvascular endothelial cells, NI: non-irradiated, I: irradiated, Gy: gray, GF: growth factors, AO: antioxidants, DPI: days post-irradiation. Created with https://BioRender.com.

irradiated (I) HBMEC in the TW were cocultured with NI NSPCs. As before, the presence of HBMEC—whether irradiated or not—resulted in an increased number of NSPCs compared to the empty TW control after 3 days of coculture. However, no significant differences in cell counts were observed between the groups with NI, 2 Gy, and 8 Gy-irradiated HBMEC (Fig. 4C).

However, when using HBMEC 10 days post-irradiation, we faced a challenge: the HBMEC could not survive beyond 3 days in the TW coculture. This was likely due to the absence of trophic factors, such as FGF or EGF, in the culture media. Adding these growth factors could have supported HBMEC survival; however, we deliberately chose not to include them, as they might interfere with the

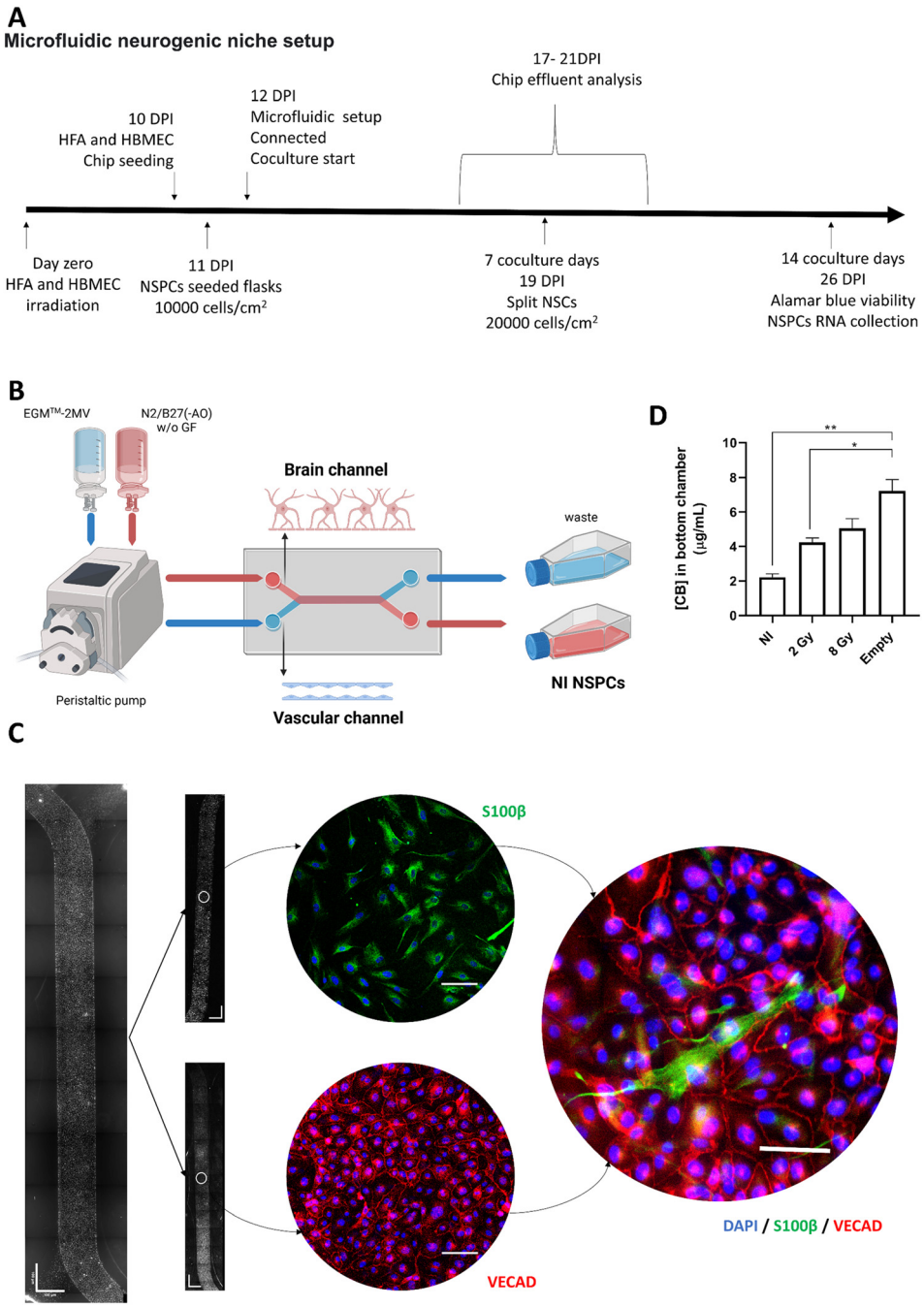


Fig. 5 Microfluidic neurogenic niche setup. (A) Experimental timelines in microfluidic neurogenic niche setup. (B) Schematic representation of the design for the microfluidic neurogenic niche model. Created with Biorender. (C) To recreate the neurogenic niche, HFA were seeded on one side of the membrane, while HBMEC were seeded on the opposite side, allowing physical interaction between the two cell types. Scale bar = 100 μm. (D) Chip permeability was measured, showing a significant decrease in permeability with cellular presence, except in the 8 Gy irradiated. HFA: human fetal astrocytes, HBMEC: human brain microvascular endothelial cells, Gy: gray, NSPCs: neural stem and progenitor cells, DPI: days post irradiation, TW: Transwell.

 

growth dynamics of the NSPCs, potentially skewing the experimental outcomes.

### Assembling the microfluidic neurogenic niche setup

Adding growth factors, such as FGF and EGF, directly to the top chamber of the Transwell to allow HBMEC survival presented a challenge, as they can diffuse into the bottom chamber where the NSPCs were cultured. This would risk unintended exposure of the NSPCs to these factors, which would influence their behavior and interfere with the interpretation of the results.

To overcome this limitation, we opted to use a microfluidic neurogenic niche setup. This system offers several key advantages over traditional Transwell setups. It is composed of separate microchannels that allow for the compartmentalization of different cell types, with control over the culture conditions in each channel. The microfluidic design improves the control of diffusion of molecules, such as growth factors, between the compartments. This is because the constant flow prevents the accumulation of factors in one compartment from passively diffusing into another. We confirm that the CB concentration in the neural chamber after 22 hours was significantly higher in the Transwell system compared to the microfluidic setup (Fig. S4). This finding highlight that the diffusion of a molecule introduced on the vascular side is more constrained in our microfluidic system than in the Transwell setup.

By using this system, we were able to maintain distinct media compositions for the HBMEC (vascular channel) and HFA (brain channel).

The experimental setup aimed to recreate the neurogenic niche, using HFA and HBMEC irradiated and cultured for 10 days to establish a persistent inflammatory profile (Fig. 5A and B). Irradiated HFA and HBMEC were seeded on opposite sides of the membrane to allow direct cell–cell interaction (Fig. 5C). During the 14-day of coculture, growth factor-depleted media from the HFA channel ("brain side") was collected to assess its effects on NI NSPCs, while the HBMEC channel ("vascular side") received media supplemented with growth factors to support endothelial cell viability. Notably, chip permeability decreased significantly in the presence of cells, demonstrating effective barrier formation (Fig. 5D).

The 14-day coculture period was not intended to model a specific clinical scenario, since chronic radiation-induced symptoms may take years to manifest in patients. However, maintaining the microfluidic system in stable conditions for such extended periods is technically unfeasible. Based on our preliminary data, we observed that 12–14 days were sufficient to induce marked morphological alterations in astrocytes and endothelial cells, as well as significant changes in their secretome. Therefore, this timepoint was selected as a practical and biologically relevant endpoint to capture the onset of radiation-induced cellular and molecular adaptations within the constraints of the *in vitro* system.

### The effluent of the microfluidic neurogenic niche setup affects NSPCs growth and gene expression

Next analysis explored how conditioned media from irradiated neurogenic niche-supporting cells could influence NI NSPCs in terms of proliferation and gene expression. We observed a notable increase in the proliferation of NI NSPCs exposed to the effluent from the 2 Gy irradiated microfluidic neurogenic niche setup (Fig. 6A and B). This was further supported by the increased RNA yield obtained from these NSPCs (Fig. 6C).

Moreover, our data revealed that exposure to the effluent from the 8 Gy-irradiated neurogenic niche significantly reduced *CD44* gene expression in NI NSPCs (Fig. 6D). Additionally, the differential gene expression patterns observed indicate a potential shift in the differentiation state of NSPCs upon exposure to irradiated effluent. Specifically, the 2 Gy-conditioned media led to an upregulation of *SOX9* expression, a transcription factor involved in NSPC maintenance and gliogenesis (Fig. 6E). In contrast, the effluent from the 8 Gy setup showed a tendency to increase *S100B* expression, a marker of astrocytic differentiation (Fig. 6F), while simultaneously decreasing *HES3* expression, a key regulator of NSPC self-renewal (Fig. 6G). These findings highlight the differential effects of radiation-damaged niche environments on NSPC fate, potentially shifting them toward astrocytic differentiation under higher radiation doses. Non-significant changes in gene expression are provided in Fig. S5.

### Inflammatory pattern of the HFA + HBMEC barriers during the microfluidic experiment

In this study, we sought to identify the components of the chip effluents responsible for eliciting the NSPC response. However, inflammatory cytokines in the effluents were below the assay's detection threshold, even after attempts to concentrate the media using a SpeedVac system. To overcome this limitation, we collected media from static conditions for subsequent analysis. Radiation exposure induced a dose-dependent modulation of the inflammatory cytokine profile within the chip's neural chamber. Both 2 Gy and 8 Gy irradiation significantly increased CCL2 levels and decreased IL-8 levels compared to non-irradiated controls. Notably, only the 8 Gy condition resulted in elevated IL-6, IFN-α2, and IL-18, indicating a more pronounced pro-inflammatory response at higher radiation doses. These findings suggest that stronger irradiation triggers a broader neuroinflammatory signature, which may contribute to downstream effects on neural cell viability (Fig. 7).

## Discussion

Cerebral radiation therapy carries a significant risk of long-term neurocognitive impairment.[2] Radiation-induced cognitive disorder is a complex, multifaceted condition that remains poorly understood. Learning and memory are

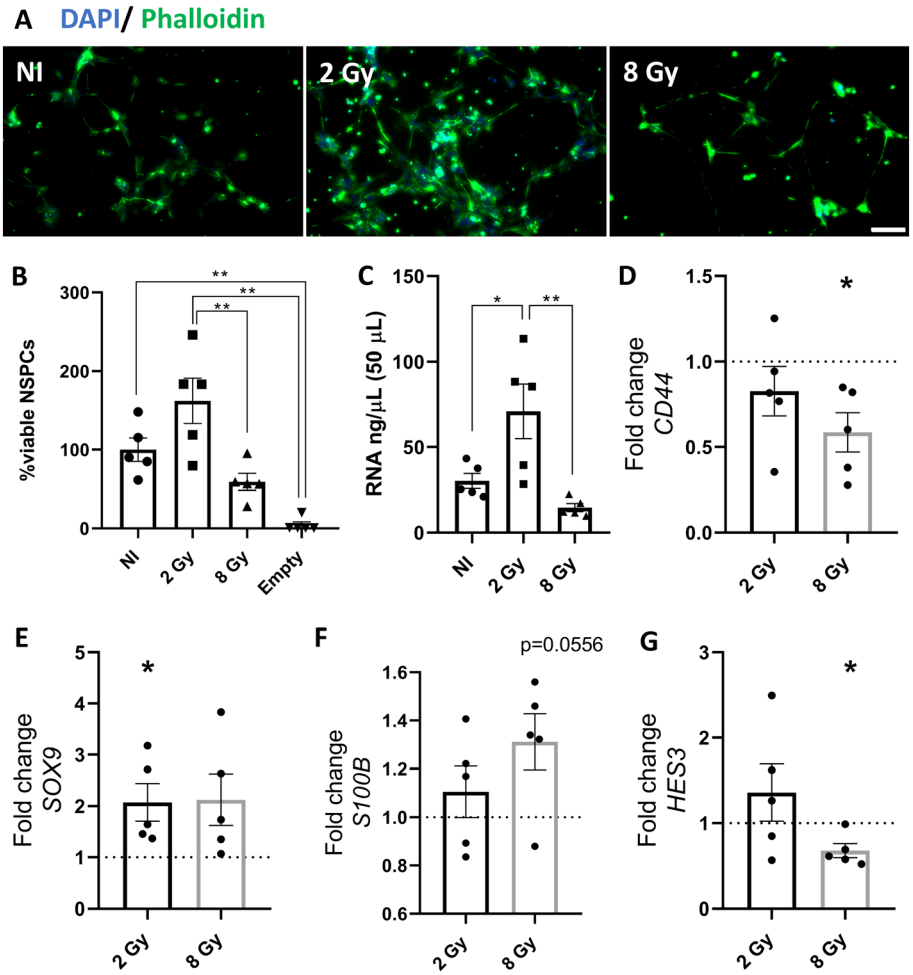


**Fig. 6** Effects of media from the microfluidic neurogenic niche on NSPCs viability, RNA yield, and gene expression after 14 days. (A) Immunocytochemistry showing the NSPCs in flasks after 14 days of receiving media from the microfluidic neurogenic niche setup. Scale bar = 100 µm. (B) NSPCs viability after 14 days of receiving media from the microfluidic neurogenic niche setup, measured by Alamar blue fluorescence. Quantification was performed by setting the fluorescence in the NI HFA/HBMEC group as 100% viable cells, with other conditions expressed as percentages relative to the NI group. $N = 5$. * = $p < 0.05$, ** = $p < 0.01$, ANOVA followed by Tukey's *post hoc* test (C) RNA yield from NSPCs in each group, confirming the Alamar Blue results. $N = 5$. * = $p < 0.05$, ** = $p < 0.01$, ANOVA followed by Tukey's *post hoc* test (D) *CD44* (E) *SOX9* (F) *S100B* and (G) *HES3* gene expression in NI NSPCs after 14 days of receiving media from the microfluidic neurogenic niche setup. qPCR results were considered statistically significant when the fold change differed from 1 (control level). $N = 5$. *$p < 0.05$ (one sample Student's *t*-test). NSPCs: neural stem and progenitor cells; NI: non-irradiated; Gy: gray; *S100B*: S100β calcium-binding protein beta; *CD44*, cluster of differentiation 44; *SOX9*: SRY-box transcription factor 9; *HES3*: hairy and enhancer of split 3.

intricately linked to neurogenesis.[24] The subgranular zone (SGZ) of the hippocampus, along with the subventricular zone (SVZ) in the lateral ventricles, houses the primary sites of adult neurogenesis.[25,26] Substantial evidence indicates that radiation therapy (RT) suppresses neurogenesis.[11] Studies in rodents have demonstrated a dose-dependent loss of neurogenesis, even with radiation doses as low as 2 Gy. Early effects are detectable as soon as 2 hours post-irradiation,[27] with proliferating SGZ cells reduced by 93–96% within 48 hours.[28,29] The irradiated SGZ area decreased significantly to 70%, 50%, and 48% of control levels seven days after exposure to 4, 8, and 12 Gy, respectively.[27] Similarly, a dose of 10 Gy reduced neurogenesis and impaired cognitive performance in maze tests.[29] In 14-day-old mice, a single dose of 8 Gy caused learning deficits shortly after irradiation, with reversal learning impairments persisting for up to one-year post-irradiation.[30,31] Notably, transplanting NSPCs into the hippocampus partially improved cognitive performance in irradiated rodents.[32,33]

Our findings reinforce the observation that NSPCs are particularly vulnerable to radiation-induced damage, as even low doses (0.5 Gy) resulted in a marked reduction in cell viability. These results are consistent with previous reports highlighting the high radiosensitivity of neural progenitors within the neurogenic niche. The NSPCs used in our study had previously been shown to retain multipotency, differentiating into both neurons and astrocytes upon withdrawal of growth factors, confirming their neurogenic capacity under baseline condition.[20,34] However, upon irradiation, we observed pronounced cell death and a

 

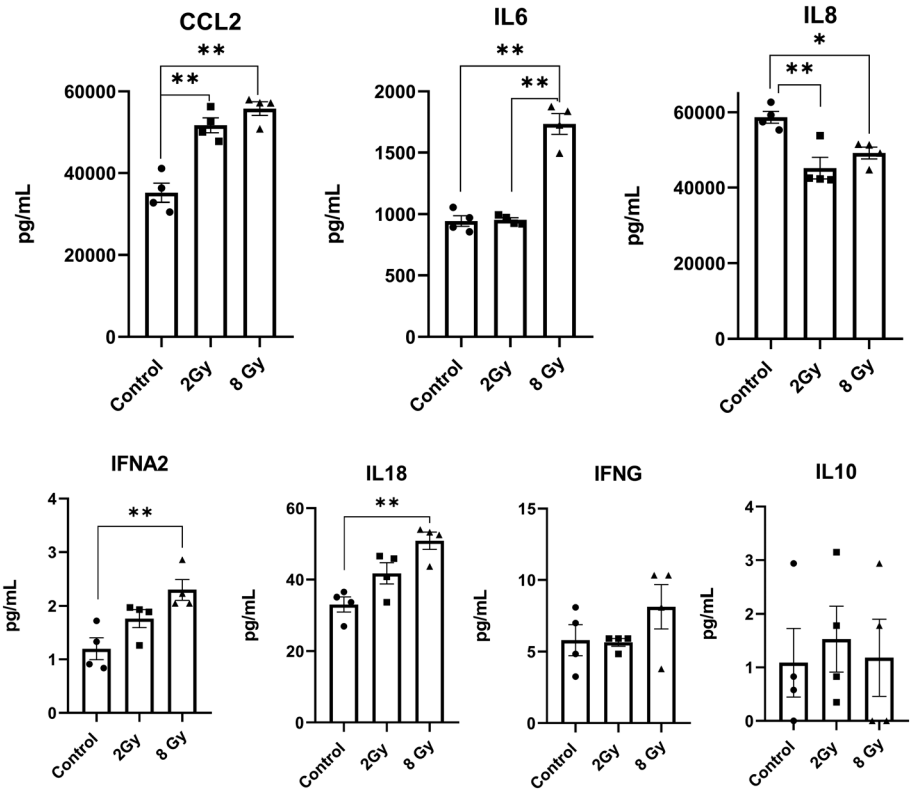


Fig. 7 Inflammatory cytokines detected in the irradiated chip neural chamber. Irradiation at both 2 Gy and 8 Gy resulted in significantly increased levels of CCL2 and decreased levels of IL-8 in the neural chamber. Notably, only the 8 Gy condition led to elevated concentrations of IL-6, IFN-$\alpha$2, and IL-18. *$p < 0.05$, **$p < 0.01$, ANOVA followed by Tukey *post hoc* test. Results from a pooled sample analyzed in quadruplicate. Statistical analysis applied on the technical replicates. CCL2: C–C motif chemokine ligand 2, IL6: interleukin 6, IL8: interleukin 8, Gy: gray.

significant loss of proliferative potential, which precluded further assessment of their differentiation profile.

In contrast, HFA and HBMEC exhibited higher viability rates under similar conditions. However, it is important to consider that the cytotoxic effects of radiation are more pronounced in actively proliferating cells. This consideration is particularly relevant for HBMEC, as the assay was conducted in 96-well plates, where endothelial cells typically form a confluent monolayer shortly after seeding. Upon reaching confluence, these cells enter a quiescent state, characterized by cell cycle arrest and reduced mitotic activity. This quiescent phenotype may have mitigated the impact of radiation, potentially masking its deleterious effects. Therefore, the proliferation status of HBMEC at the time of irradiation could have influenced the observed outcomes.

We observed pronounced astrocyte hypertrophy[35] and a marked increase in ICAM expression, indicating the acquisition of an inflammatory profile in these cells.[36] Radiation also altered cytokine expression patterns in HFA: *IL1B* was highly expressed in 8 Gy-irradiated HFA during the first 24 hours post-irradiation but was subsequently replaced by elevated *IL6* expression over a 14-day period. Similarly, 8 Gy-irradiated HBMEC became hypertrophic and exhibited increased expression of *IL6* at 24 hours and *IL1B* at 14 days.

Beyond direct radiation damage, other mechanisms, such as the bystander effect—where irradiated cells secrete factors that influence surrounding cells—may also impair neurogenesis.[37] To better understand these mechanisms, we characterized how NSPCs respond to the inflammatory microenvironment created by HFA and HBMEC.

To investigate this, we studied the influence of co-culturing non-irradiated (NI) NSPCs with irradiated (I) HFA using a TW model. The presence of HFA, whether irradiated or not, increased the number of viable NSPCs in all conditions compared to the acellular control (empty TW without HFA). Notably, NSPCs cocultured with 8 Gy irradiated HFA showed an even greater increase in numbers during the first three days compared to those cocultured with NI HFA. This highlights the dual role of inflammation in NSPCs: it can either promote or inhibit proliferation, survival, or differentiation depending on factors such as the timing, involved cell types, and chronicity of the inflammatory response.[38,39] When the same protocol was repeated using HBMEC instead of HFA, the mere presence of HBMEC similarly enhanced NSPCs viability. However, no significant differences were observed between NSPCs cocultured with NI or irradiated HBMEC.

To assess whether NSPCs would sustain this pattern over time, HFA were irradiated (2 Gy or 8 Gy) and cultured for 10 days to develop a persistent inflammatory profile. Cocultures were then extended, and NSPCs were observed for 14 days. By this time point, NSPCs cocultured with 8 Gy irradiated HFA

showed a decline in numbers, no longer differing from the acellular control condition. This could suggest that, unlike an immediate response (represented in the 3-day experiment), in a more prolonged scenario, the exposure of NSPCs to an inflammatory secretome over an extended period might, instead of stimulating cell proliferation, lead to its depletion.

However, the static TW approach presented several challenges: 1) we could not keep HBMEC in a growth factor-depleted media more than three days because of cell death, 2) The initial seeding density of NSPCs is difficult to define: usually, NSPCs have a high proliferation rate, reaching confluency in the first days (which has to be avoided to identify differences among the groups). However, in a media without growth factors, NSPCs start to die after day 3 (Fig. S1). To overcome these issues, we designed our microfluidic neurogenic niche setup. This model allowed us to overcome the stated difficulties above by 1) using different types of media in the different channels, allowing us to feed HBMEC with growth factors with a minor influence in the NSPCs system, and 2) by connecting the chip with the NSPCs flask we could maintain the cells receiving the irradiated cell-conditioned media, while being able to split and control cell density in the flask, allowing for better insights. Contrary to our TW approach, NSPCs reacted differently to the 2 Gy- and 8 Gy CI chips' effluents in this setup: while the 2 Gy chip media increased NSPCs viability (confirmed by both Alamar Blue assay and RNA amount), the 8 Gy CI chip media had an opposite effect on NSPCs viability.

The expression profiles of NSPCs exposed to conditioned media from irradiated cells also varied according to the radiation dose. Notably, effluents derived from cells subjected to 2 Gy irradiation induced a pronounced upregulation of *SOX9*, a transcription factor critical for NSPC maintenance and gliogenesis.[40] Conversely, conditioned media from the 8 Gy-irradiated setup tended to increase the expression of *S100B*, a well-established astrocytic differentiation marker, reinforcing the idea that radiation may bias NSPCs toward a glial lineage.[41] *SOX9* functions as a key transcription factor for the specification and maintenance of multipotent NSPCs, promoting the transition from a neurogenic to a gliogenic state and facilitating the generation of astrocytes and oligodendrocytes.[42–45] Elevated *SOX9* levels are associated with both enhanced self-renewal and the maintenance of an undifferentiated phenotype, while also predisposing cells toward glial fate commitment.[42–46] *S100B*, in turn, is predominantly expressed by astrocytes and oligodendrocytes and plays important roles in the regulation of their differentiation, growth, and maturation during brain development. The upregulation of *S100B* in NSPCs suggests activation of astroglial maturation programs, potentially triggered by environmental stimuli or injury-related cues, and is further implicated in neurotrophic and neuroprotective processes.[41,47] Taken together, these findings suggest that soluble factors released by irradiated cells may influence NSPCs fate decisions in a dose-dependent manner—maintaining stemness and gliogenic potential at lower doses, while promoting astrocytic differentiation under higher radiation stress. Such dose-sensitive responses could have implications for understanding how radiation reshapes the neurogenic niche and contributes to glial remodeling in the injured brain.

Simultaneously, a decrease in *HES3* expression was observed in response to 8 Gy-conditioned media. Since *HES3* is a critical regulator of NSPCs self-renewal, its downregulation could indicate a potential depletion of the neural stem cell niche.[48–51] An intriguing finding of this study is the down-regulation of *CD44* expression in NSPCs exposed to 8 Gy-conditioned media. CD44, the principal surface receptor for hyaluronic acid (HA), plays a pivotal role in various cellular processes, including motility, signal transduction, and intercellular as well as cell–matrix adhesion.[52] Notably, *CD44* is expressed by both glial and neuronal cells, underscoring its functional importance across multiple CNS cell types.[52]

These findings are consistent with previous reports showing that radiation affects neurogenesis not only through direct cytotoxicity but also *via* radiation-induced bystander effects mediated by irradiated niche cells. For example, conditioned media or co-culture with irradiated endothelial (bEnd.3)[7] or glioma (GL261)[53] cells significantly reduce NSPC proliferation, neurosphere formation, and differentiation capacity, even without direct irradiation, ultimately leading to impaired hippocampal neurogenesis and cognitive dysfunction *in vivo*. Mechanistically, irradiated glioblastoma cells have been shown to secrete cytokines such as IL-8, TGF-β1, IL-6, and TRAIL, which induce apoptosis and selectively suppress neuronal, but not astroglial, differentiation of non-irradiated NSPCs.[54] Together, these observations suggest that radiation disrupts the entire neurogenic progression—from NSPCs to mature neurons, astrocytes, and oligodendrocytes—through both direct damage and bystander effect-mediated intercellular signaling within the neurogenic niche.

In this study, we aimed to identify the components of the chip effluents responsible for triggering the NSPC response. However, inflammatory cytokines in the effluents were below the assay's detection threshold, and attempts to concentrate the media using a SpeedVac system did not overcome this limitation. To enhance sensitivity, we collected effluents under static conditions. Under these conditions, we observed that media from the 8 Gy-irradiated chips contained elevated levels of pro-inflammatory cytokines, including IL6, TNFA2, and TNFG. These inflammatory changes correlate with our observations of reduced NSC viability in response to 8 Gy chip effluents, suggesting that the pro-inflammatory milieu generated under high-dose irradiation may be a key contributor to the observed cytotoxicity. Notably, IL8 levels were reduced in both irradiated chips. One important aspect of our model is that HFA and HBMEC were irradiated in plates and transferred to the chip 10 days later, at which point viability was approximately 70–80% for 2 Gy and 50% for 8 Gy. It is possible that highly damaged cells—which

 

could release substantial amounts of inflammatory mediators —were lost during this transfer, potentially underestimating the true inflammatory burden. Nevertheless, the cytokine profile from the 8 Gy condition aligns with the reduced NSPCs viability, reinforcing the link between radiation-induced neuroinflammation and stem cell vulnerability.

Interestingly, at 14 DPI, HFA exposed to 2 Gy exhibited a significant upregulation of *IL10*, a well-characterized anti-inflammatory cytokine implicated in central nervous system repair and neuroprotection.[56] IL10 plays a critical role in dampening inflammation and promoting tissue regeneration.[57,58] Although elevated IL10 levels were not detected in the 2 Gy chip effluent, its increased expression in the irradiated cells suggests a shift toward a neuroprotective, pro-repair phenotype. Consistent with this interpretation, recent findings demonstrate that activated regulatory T cells (Tregs) NSPCs proliferation in the SVZ *via* IL-10-dependent mechanisms, whereas IL10 blockade redirects NSPCs fate toward astroglial differentiation ($Mash1^+/GFAP^+$ ratio).[59] This supports the notion that IL10 acts as a central modulator of the balance between NSPCs proliferation and glial activation. Similarly, neuronal IL10 expression delivered *via* AAV vectors has been shown to attenuate microglial activation, reduce gliosis, enhance neurogenesis, and improve cognitive performance in Alzheimer's disease models.[60] Together, these findings suggest that the 2 Gy irradiation may elicit a controlled anti-inflammatory response mediated by IL-10, fostering a microenvironment conducive to NSPCs survival and regeneration.

In physiological conditions, interstitial flow rates in the rodent brain parenchyma are estimated at approximately 0.1–0.3 $\mu L\ min^{-1}\ g^{-1}$, with fluid movement occurring mainly along perivascular spaces and axonal tracts.[55] We therefore acknowledge that the absolute flow velocities in our device do not exactly reproduce the very slow bulk interstitial flow measured *in vivo*. However, the higher perfusion rate used here (1 $\mu L\ min^{-1}$, residence time in brain channel of some minutes) was primarily determined by the technical limitations of the pumping system and the need to maintain stable fluid circulation and nutrient exchange over prolonged culture periods. In addition, the chosen rate ensured adequate convective transport across the membrane and cell compartments, allowing for the establishment of soluble-factor gradients and minimizing bubble formation or channel obstruction. Another important technical consideration is that in our microfluidic setup, perfusion occurs equally across both the vascular and perivascular compartments. Although this does not fully recapitulate the compartmentalized fluid dynamics of the *in vivo* brain microenvironment, it was necessary for the practical constraints of our model.

Another limitation of our study is the absence of microglia in our model. Microglia play a pivotal role in the brain's response to radiation, serving as key regulators of neuroinflammation, tissue repair, and neural homeostasis.[61,62] The lack of microglia in our experimental setup presents a significant limitation, as their dynamic interactions with other brain cells, particularly in the context of radiation-induced injury, are likely to affect both gene expression profiles and functional outcomes.[63] Microglia-derived molecules have a strong influence on astrocyte activation and, consequently, on the broader inflammatory and trophic environment. As highlighted by recent studies, the bidirectional crosstalk between microglia and astrocytes can either exacerbate or attenuate neuroinflammation depending on the stimuli and molecular context.[64,65] Including microglia in the model would therefore be expected to alter cytokine signaling substantially which can modulate astrocytic and NSPCs behavior. While incorporating microglia into future models will achieve a more comprehensive understanding of the brain's cellular and molecular responses to radiation, our studies point to the additional importance of the brain microvascular endothelial cells and astrocytes.

## Conclusions

This study highlights the utility of a novel neurogenic chip setup to model and dissect the complex interactions between radiation exposure and the human neurogenic niche. By integrating irradiated astrocytes and brain microvascular endothelial cells with neural stem and progenitor cells (NSPCs) in a dynamic microphysiological environment, we were able to recapitulate key features of radiation-induced neuroinflammation and its effects on NSPCs viability, proliferation, and gene expression. Our data demonstrate that not only the presence, but also the intensity and composition of the inflammatory response—particularly under high-dose irradiation—critically influence NSPCs behavior. Importantly, the model captures cell–cell and cell–environment dynamics that are absent in static systems, underscoring its value for mechanistic studies and therapeutic screening. These findings establish the neurogenic chip setup as a powerful platform for investigating radiation-induced neural injury and for guiding the development of targeted strategies to mitigate long-term neurocognitive sequelae.

## Author contributions

LNZ: conceptualized the study, performed the experiments and the analyses, wrote the original draft, and reviewed and edited the document table and figures; JR: advised the execution of the experiments and analyses, and reviewed the final document; PN: advised the execution of the experiments and analyses, and reviewed and edited the final document; KB: advised the execution of the experiments and analyses, and reviewed and edited the final document; MAP: advised the execution of the experiments and analyses, reviewed and edited the final document; AH: conceptualized the study, advised the execution of the experiments and analyses,

reviewed and edited the final document. All authors have read and agreed to the final version of the manuscript.

## Conflicts of interest

The authors declare that they have no competing interests.

## Abbreviations

| | |
|---|---|
| AM | Astrocyte media |
| AO | Antioxidants |
| AU | Arbitrary units |
| BBB | Blood–brain barrier |
| CB | Cascade Blue |
| cDNA | Complementary DNA |
| CNS | Central nervous system |
| Ct | Threshold cycle |
| DAPI | 4′,6′-Diamidino-2-phenylindole |
| DPI | Days post-irradiation |
| DPBS | Dulbecco's phosphate-buffered saline |
| DTI | Defined trypsin inhibitor |
| EGM | Endothelial cell growth medium |
| FBS | Fetal bovine serum |
| Gy | Gray (unit of radiation dose) |
| HFA | Human fetal astrocytes |
| HBMEC | Human brain microvascular endothelial cells |
| HPI | Hours post-irradiation |
| I | Irradiated |
| mRNA | Messenger RNA |
| MV | Microvascular |
| NI | Non-irradiated |
| NSPCs | Neural stem andprogenitor cells |
| PCR | Polymerase chain reaction |
| PFA | Paraformaldehyde |
| PDMS | Polydimethylsiloxane |
| PET | Polyethylene terephthalate |
| RPM | Revolutions per minute |
| RT | Radiation therapy |
| SGZ | Subgranular zone |
| SVZ | Subventricular zone |
| TW | Transwell |

## Data availability

The datasets generated and analyzed during the current study are available in https://doi.org/10.6084/m9.figshare.29097848.

Supplementary information (SI) is available. See DOI: https://doi.org/10.1039/d5lc00498e.

## Acknowledgements

LNZ acknowledges funding from the São Paulo Research Foundation (FAPESP), grant numbers 2021/14327-8 and 2022/16296-5, and the National Council for Scientific and Technological Development (CNPq), grant number 202895/2019-0. AH acknowledges funding from Hjärnfonden 2022-0151, Swedish Research Council 2022-01362, 2019-01803, and Knut and Alice Wallenberg Stiftelse 2015.0178, 2020.0206. "This work was supported by AIMES – Center for the Advancement of Integrated Medical and Engineering Sciences (https://www.aimes.se), Karolinska Institutet (1-249/2019), KTH Royal Institute of Technology (VF-2019-0110) and Getinge AB (4-1599/2018)". We thank the iPS core, the Biomedicum Imaging Core (BIC) and the X-ray Irradiation Core Facility at Karolinska Institute for access to their service. We thank Sofia Skyttner, Medical Physicist, for the X-ray recipes calculations. JR acknowledges funding by the European Union (HORIZON-MSCA-2022-PF-01, GA-101109010-NEoC).

## References

1 K. D. Miller, Q. T. Ostrom and C. Kruchko, *et al.*, Brain and other central nervous system tumor statistics, *Ca-Cancer J. Clin.*, 2021, **71**, 381–406, DOI: 10.3322/caac.21693.

2 S. Pazzaglia, G. Briganti and M. Mancuso, *et al.*, Neurocognitive Decline Following Radiotherapy: Mechanisms and Therapeutic Implications, *Cancers*, 2020, **12**, 20200108, DOI: 10.3390/cancers12010146.

3 T. Calimeri, F. Marcucci and A. Corti, Overcoming the blood-brain barrier in primary central nervous system lymphoma: a review on new strategies to solve an old problem, *Ann. Lymphoma*, 2021, **5**, 20, DOI: 10.21037/aol-20-54.

4 E. B. Ludmir, D. R. Grosshans and K. D. Woodhouse, Radiotherapy Advances in Pediatric Neuro-Oncology, *Bioengineering*, 2018, **5**, 20181104, DOI: 10.3390/bioengineering5040097.

5 C. Turnquist, B. T. Harris and C. C. Harris, Radiation-induced brain injury: current concepts and therapeutic strategies targeting neuroinflammation, *Neurooncol. Adv.*, 2020, **2**(1), vdaa057, DOI: 10.1093/noajnl/vdaa057.

6 S. Saad and T. J. Wang, Neurocognitive Deficits After Radiation Therapy for Brain Malignancies, *Am. J. Clin. Oncol.*, 2015, **38**, 634–640, DOI: 10.1097/COC.0000000000000158.

7 L. Ma, Z. Ye and Y. Zhang, *et al.*, Irradiated microvascular endothelial cells may induce bystander effects in neural stem cells leading to neurogenesis inhibition, *J. Radiat. Res.*, 2022, **63**, 192–201, DOI: 10.1093/jrr/rrab125.

8 J. M. Butler, S. R. Rapp and E. G. Shaw, Managing the cognitive effects of brain tumor radiation therapy, *Curr. Treat. Options Oncol.*, 2006, **7**, 517–523, DOI: 10.1007/s11864-006-0026-5.

9 V. Gondi, W. A. Tomé and M. P. Mehta, Why avoid the hippocampus? A comprehensive review, *Radiother. Oncol.*, 2010, **97**(370–376), 20101020, DOI: 10.1016/j.radonc.2010.09.013.

10 G. Zanni, S. Goto and A. F. Fragopoulou, *et al.*, Lithium treatment reverses irradiation-induced changes in rodent neural progenitors and rescues cognition, *Mol. Psychiatry*, 2021, **26**(322–340), 20191114, DOI: 10.1038/s41380-019-0584-0.

11 M. T. Makale, C. R. McDonald and J. A. Hattangadi-Gluth, *et al.*, Mechanisms of radiotherapy-associated

 

cognitive disability in patients with brain tumours, *Nat. Rev. Neurol.*, 2017, **13**(52–64), 20161216, DOI: 10.1038/nrneurol.2016.185.

12 F. Ferraro, C. L. Celso and D. Scadden, Adult stem cels and their niches, *Adv. Exp. Med. Biol.*, 2010, **695**, 155–168, DOI: 10.1007/978-1-4419-7037-4_11.

13 J. Schneider, J. Karpf and R. Beckervordersandforth, Role of Astrocytes in the Neurogenic Niches, *Methods Mol. Biol.*, 2019, **1938**, 19–33, DOI: 10.1007/978-1-4939-9068-9_2.

14 M. Sawada, M. Matsumoto and K. Sawamoto, Vascular regulation of adult neurogenesis under physiological and pathological conditions, *Front. Neurosci.*, 2014, **8**(53), 20140317, DOI: 10.3389/fnins.2014.00053.

15 F. Ehret, S. Vogler and G. Kempermann, A co-culture model of the hippocampal neurogenic niche reveals differential effects of astrocytes, endothelial cells and pericytes on proliferation and differentiation of adult murine precursor cells, *Stem Cell Res.*, 2015, **15**(514–521), 20150926, DOI: 10.1016/j.scr.2015.09.010.

16 E. I. Azzam, J. P. Jay-Gerin and D. Pain, Ionizing radiation-induced metabolic oxidative stress and prolonged cell injury, *Cancer Lett.*, 2012, **327**(48–60), 20111217, DOI: 10.1016/j.canlet.2011.12.012.

17 S. Maynard, E. F. Fang and M. Scheibye-Knudsen, *et al.*, DNA Damage, DNA Repair, Aging, and Neurodegeneration, *Cold Spring Harbor Perspect. Med.*, 2015, **5**, 20150918, DOI: 10.1101/cshperspect.a025130.

18 A. R. Davalos, J. P. Coppe and J. Campisi, *et al.*, Senescent cells as a source of inflammatory factors for tumor progression, *Cancer Metastasis Rev.*, 2010, **29**, 273–283, DOI: 10.1007/s10555-010-9220-9.

19 S. M. Chambers, C. A. Fasano and E. P. Papapetrou, *et al.*, Highly efficient neural conversion of human ES and iPS cells by dual inhibition of SMAD signaling, *Nat. Biotechnol.*, 2009, **27**(275–280), 20090301, DOI: 10.1038/nbt.1529.

20 A. Falk, P. Koch and J. Kesavan, *et al.*, Capture of neuroepithelial-like stem cells from pluripotent stem cells provides a versatile system for in vitro production of human neurons, *PLoS One*, 2012, **7**(e29597), 20120117, DOI: 10.1371/journal.pone.0029597.

21 K. J. Livak and T. D. Schmittgen, Analysis of relative gene expression data using real-time quantitative PCR and the 2(-Delta Delta C(T)) Method, *Methods*, 2001, **25**, 402–408, DOI: 10.1006/meth.2001.1262.

22 S. Mader and L. Brimberg, Aquaporin-4 Water Channel in the Brain and Its Implication for Health and Disease, *Cell*, 2019, **8**, 20190127, DOI: 10.3390/cells8020090.

23 Q. Dasgupta, A. Jiang and A. M. Wen, *et al.*, A human lung alveolus-on-a-chip model of acute radiation-induced lung injury, *Nat. Commun.*, 2023, **14**(6506), 20231016, DOI: 10.1038/s41467-023-42171-z.

24 D. N. Abrous and J. M. Wojtowicz, Interaction between Neurogenesis and Hippocampal Memory System: New Vistas, *Cold Spring Harbor Perspect. Biol.*, 2015, **7**, 20150601, DOI: 10.1101/cshperspect.a018952.

25 L. E. Jarrard, On the role of the hippocampus in learning and memory in the rat, *Behav. Neural Biol.*, 1993, **60**, 9–26, DOI: 10.1016/0163-1047(93)90664-4.

26 A. Alvarez-Buylla and D. A. Lim, For the long run: maintaining germinal niches in the adult brain, *Neuron*, 2004, **41**, 683–686.

27 H. Fukuda, A. Fukuda and C. Zhu, *et al.*, Irradiation-induced progenitor cell death in the developing brain is resistant to erythropoietin treatment and caspase inhibition, *Cell Death Differ.*, 2004, **11**, 1166–1178, DOI: 10.1038/sj.cdd.4401472.

28 S. Mizumatsu, M. L. Monje and D. R. Morhardt, *et al.*, Extreme sensitivity of adult neurogenesis to low doses of X-irradiation, *Cancer Res.*, 2003, **63**, 4021–4027.

29 J. Raber, R. Rola and A. LeFevour, *et al.*, Radiation-induced cognitive impairments are associated with changes in indicators of hippocampal neurogenesis, *Radiat. Res.*, 2004, **162**, 39–47, DOI: 10.1667/rr3206.

30 N. Karlsson, M. Kalm and M. K. Nilsson, *et al.*, Learning and activity after irradiation of the young mouse brain analyzed in adulthood using unbiased monitoring in a home cage environment, *Radiat. Res.*, 2011, **175**(336–346), 20101228, DOI: 10.1667/rr2231.1.

31 M. Kalm, N. Karlsson and M. K. Nilsson, *et al.*, Loss of hippocampal neurogenesis, increased novelty-induced activity, decreased home cage activity, and impaired reversal learning one year after irradiation of the young mouse brain, *Exp. Neurol.*, 2013, **247**(402–409), 20130116, DOI: 10.1016/j.expneurol.2013.01.006.

32 M. M. Acharya, L. A. Christie and M. L. Lan, *et al.*, Human neural stem cell transplantation ameliorates radiation-induced cognitive dysfunction, *Cancer Res.*, 2011, **71**(4834–4845), 20110714, DOI: 10.1158/0008-5472.CAN-11-0027.

33 Y. Sato, N. Shinjyo and M. Sato, *et al.*, Grafting Neural Stem and Progenitor Cells Into the Hippocampus of Juvenile, Irradiated Mice Normalizes Behavior Deficits, *Front. Neurol.*, 2018, **9**(715), 20180911, DOI: 10.3389/fneur.2018.00715.

34 A. Marin Navarro, R. J. Pronk and A. T. van der Geest, *et al.*, p53 controls genomic stability and temporal differentiation of human neural stem cells and affects neural organization in human brain organoids, *Cell Death Dis.*, 2020, **11**(52), 20200123, DOI: 10.1038/s41419-019-2208-7.

35 M. Kalm, A. Fukuda and H. Fukuda, *et al.*, Transient inflammation in neurogenic regions after irradiation of the developing brain, *Radiat. Res.*, 2009, **171**, 66–76, DOI: 10.1667/rr1269.1.

36 T. M. Bui, H. L. Wiesolek and R. Sumagin, ICAM-1: A master regulator of cellular responses in inflammation, injury resolution, and tumorigenesis, *J. Leukocyte Biol.*, 2020, **108**(787–799), 20200317, DOI: 10.1002/jlb.2mr0220-549r.

37 R. Baskar, Emerging role of radiation induced bystander effects: Cell communications and carcinogenesis, *Genome Integr.*, 2010, **1**(13), 20100912, DOI: 10.1186/2041-9414-1-13.

38 S. Das and A. Basu, Inflammation: a new candidate in modulating adult neurogenesis, *J. Neurosci. Res.*, 2008, **86**, 1199–1208, DOI: 10.1002/jnr.21585.

39 P. A. Carpentier and T. D. Palmer, Immune influence on adult neural stem cell regulation and function, *Neuron*, 2009, **64**, 79–92, DOI: 10.1016/j.neuron.2009.08.038.
40 P. Kang, H. K. Lee and S. M. Glasgow, *et al.*, Sox9 and NFIA coordinate a transcriptional regulatory cascade during the initiation of gliogenesis, *Neuron*, 2012, **74**, 79–94, DOI: 10.1016/j.neuron.2012.01.024.
41 K. Hernández-Ortega, A. A. Canul-Euan and J. M. Solis-Paredes, *et al.*, S100B actions on glial and neuronal cells in the developing brain: an overview, *Front. Neurosci.*, 2024, **18**(1425525), 20240704, DOI: 10.3389/fnins.2024.1425525.
42 C. E. Scott, S. L. Wynn and A. Sesay, *et al.*, SOX9 induces and maintains neural stem cells, *Nat. Neurosci.*, 2010, **13**, 1181–1189, DOI: 10.1038/nn.2646.
43 M. Wegner and C. C. Stolt, From stem cells to neurons and glia: a Soxist's view of neural development, *Trends Neurosci.*, 2005, **28**(583–588), 20050831, DOI: 10.1016/j.tins.2005.08.008.
44 S. Reiprich and M. Wegner, From CNS stem cells to neurons and glia: Sox for everyone, *Cell Tissue Res.*, 2015, **359**(111–124), 20140604, DOI: 10.1007/s00441-014-1909-6.
45 L. Pevny and M. Placzek, SOX genes and neural progenitor identity, *Curr. Opin. Neurobiol.*, 2005, **15**, 7–13, DOI: 10.1016/j.conb.2005.01.016.
46 P. C. Wei, A. Chao and H. H. Peng, *et al.*, SOX9 as a Predictor for Neurogenesis Potentiality of Amniotic Fluid Stem Cells, *Stem Cells Transl. Med.*, 2014, **3**(1138–1147), 20140825, DOI: 10.5966/sctm.2014-0019.
47 L. Rodrigues, K. M. Wartchow and M. Buchfelder, *et al.*, Longterm Increased S100B Enhances Hippocampal Progenitor Cell Proliferation in a Transgenic Mouse Model, *Int. J. Mol. Sci.*, 2022, **23**, 20220824, DOI: 10.3390/ijms23179600.
48 N. Hu and L. Zou, Multiple functions of Hes genes in the proliferation and differentiation of neural stem cells, *Ann. Anat.*, 2022, **239**, 151848, DOI: 10.1016/j.aanat.2021.151848.
49 P. Nikolakopoulou, S. W. Poser and J. Masjkur, *et al.*, STAT3-Ser/Hes3 Signaling: A New Molecular Component of the Neuroendocrine System?, *Horm. Metab. Res.*, 2016, **48**(77–82), 20160119, DOI: 10.1055/s-0041-111699.
50 R. Kageyama, T. Ohtsuka and J. Hatakeyama, *et al.*, Roles of bHLH genes in neural stem cell differentiation, *Exp. Cell Res.*, 2005, **306**, 343–348, DOI: 10.1016/j.yexcr.2005.03.015.
51 R. Kageyama, T. Ohtsuka and T. Kobayashi, Roles of Hes genes in neural development, *Dev., Growth Differ.*, 2008, **50**(Suppl 1), S97–S103, DOI: 10.1111/j.1440-169X.2008.00993.x.
52 J. Dzwonek and G. M. Wilczynski, CD44: molecular interactions, signaling and functions in the nervous system, *Front. Cell. Neurosci.*, 2015, **9**(175), 20150507, DOI: 10.3389/fncel.2015.00175.
53 X. Yang, L. Ma and Z. Ye, *et al.*, Radiation-induced bystander effects may contribute to radiation-induced cognitive impairment, *Int. J. Radiat. Biol.*, 2021, **97**(329–340), 20210111, DOI: 10.1080/09553002.2021.1864498.
54 V. N. Ivanov and T. K. Hei, Radiation-induced glioblastoma signaling cascade regulates viability, apoptosis and differentiation of neural stem cells (NSC), *Apoptosis*, 2014, **19**, 1736–1754, DOI: 10.1007/s10495-014-1040-x.
55 N. J. Abbott, Evidence for bulk flow of brain interstitial fluid: significance for physiology and pathology, *Neurochem. Int.*, 2004, **45**, 545–552, DOI: 10.1016/j.neuint.2003.11.006.
56 D. Lobo-Silva, G. M. Carriche and A. G. Castro, *et al.*, Balancing the immune response in the brain: IL-10 and its regulation, *J. Neuroinflammation*, 2016, **13**, 297, DOI: 10.1186/s12974-016-0763-8.
57 A. J. Ciciriello, D. R. Smith and M. K. Munsell, *et al.*, IL-10 lentivirus-laden hydrogel tubes increase spinal progenitor survival and neuronal differentiation after spinal cord injury, *Biotechnol. Bioeng.*, 2021, **118**(2609–2625), 20210423, DOI: 10.1002/bit.27781.
58 C. Patilas, I. Varsamos and A. Galanis, *et al.*, The Role of Interleukin-10 in the Pathogenesis and Treatment of a Spinal Cord Injury, *Diagnostics*, 2024, **14**, 20240109, DOI: 10.3390/diagnostics14020151.
59 J. Wang, L. Xie and C. Yang, *et al.*, Activated regulatory T cell regulates neural stem cell proliferation in the subventricular zone of normal and ischemic mouse brain through interleukin 10, *Front. Cell. Neurosci.*, 2015, **9**(361), 20150914, DOI: 10.3389/fncel.2015.00361.
60 T. Kiyota, K. L. Ingraham and R. J. Swan, *et al.*, AAV serotype 2/1-mediated gene delivery of anti-inflammatory interleukin-10 enhances neurogenesis and cognitive function in APP +PS1 mice, *Gene Ther.*, 2012, **19**(724–733), 20110915, DOI: 10.1038/gt.2011.126.
61 Y. Wang, J. Tian and D. Liu, *et al.*, Microglia in radiation-induced brain injury: Cellular and molecular mechanisms and therapeutic potential, *CNS Neurosci. Ther.*, 2024, **30**, e14794, DOI: 10.1111/cns.14794.
62 O.'B. M. Kerry, Microglia: Rheostats of space radiation effects in the CNS microenvironment, *Adv. Space Res.*, 2022, **35**(180–186), 20220809, DOI: 10.1016/j.lssr.2022.08.002.
63 A. M. Osman, Y. Sun and T. C. Burns, *et al.*, Radiation Triggers a Dynamic Sequence of Transient Microglial Alterations in Juvenile Brain, *Cell Rep.*, 2020, **31**, 107699, DOI: 10.1016/j.celrep.2020.107699.
64 A. Bhusal, R. Afridi and W. H. Lee, *et al.*, Bidirectional Communication Between Microglia and Astrocytes in Neuroinflammation, *Curr. Neuropharmacol.*, 2023, **21**, 2020–2029, DOI: 10.2174/1570159x21666221129121715.
65 S. H. Chen, E. A. Oyarzabal and Y. F. Sung, *et al.*, Microglial regulation of immunological and neuroprotective functions of astroglia, *Glia*, 2015, **63**(118–131), 20140813, DOI: 10.1002/glia.22738.